有机化学 DOI: 10.6023/cjoc202208039 综述与进展
Chinese Journal of Organic Chemistry REVIEW

光/电催化下 2-芳基-2*H*-吲唑 C-3 位的官能团化反应

王丹凤[a] 汪 瑾[a] 马春华*,[a] 姜玉钦*,[a] 於 兵*,[b]
([a]河南师范大学化学化工学院 河南新乡 453007)
([b]郑州大学化学学院 郑州 450001)

摘要 2*H*-吲唑是一种广泛存在于多种上市药物和活性分子中的优势骨架, 对其骨架直接进行C—H键官能团化是构建其衍生物的有效方法之一, 已经成为当前合成化学和药物化学的研究热点. 相比传统的合成方法, 可见光/电化学促进的合成方法条件温和, 是一种环境友好的合成策略. 本文以催化体系分类, 综述了近年来光/电催化下 2-芳基-2*H*-吲唑C-3 位的官能团化反应, 特别强调相应的反应机理, 为进一步开发新型的催化方法奠定基础.
关键词 2*H*-吲唑; 官能团化; 光催化; 电催化

C-3 Functionalization of 2-Aryl-2*H*-indazoles under Photo/Electrocatalysis

Wang, Danfeng[a] Wang, Jin[a] Ma, Chunhua*,[a] Jiang, Yuqin*,[a] Yu, Bing*,[b]
([a] *School of Chemistry and Chemical Engineering*, *Henan Normal University*, *Xinxiang*, *Henan 453007*)
([b] *College of Chemistry*, *Zhengzhou University*, *Zhengzhou 450001*)

Abstract 2*H*-Indazole is a privileged scaffold widely existing in drugs and bioactive molecules. The C—H functionalization of 2*H*-indazole is the cutting edge in medicinal chemistry and organic chemistry. Compared with traditional synthetic methods, the visible light/electrochemical-promoted synthetic method has mild conditions and is an environmentally friendly synthetic strategy. The C—H functionalization of 2-aryl-2*H*-indazoles at the C-3 position catalyzed by photochemical/electrochemical strategies in recent years is summarized in terms of catalytic systems, with special emphasis on the corresponding reaction mechanism, which might inspire the further development of new catalytic methods.
Keywords 2*H*-indazole; functionalization; photocatalysis; electrocatalysis

1 Introduction

As an effective bioisostere of indoles and benzimidazoles, 2*H*-indazoles have great significance in the field of drug development. By forming the π-π stacked hydrophobic interaction with the key amino acid residues (histidine and phenylalanine, *etc*.) and the hydrogen bonding interaction with the key amino acid residues (serine and tyrosine, *etc*.) in the target, the binding affinity and selectively against the target of the compound could be improved. So, it acts as an important privileged scaffold that widely exists in the drugs and bioactive molecules (Figure 1). For example, the poly(ADP-ribose)polymerase inhibitor Niraparib has been approved to treat advanced epithelial ovarian carcinoma, carcinoma of the fallopian tube, and primary peritoneal carcinoma.[1] The vascular endothelial growth factor receptor (VEGFR) inhibitor Pazopanib is a first-line drug to treat advanced renal cell carcinoma.[2] The 3C-like protease ($3CL^{pro}$) inhibitor S-217622 exhibits antiviral activity in the phase II clinical trial against the coronavirus disease 2019 (COVID-19). Oxadiazolylindazole possesses neuroprotective activity toward hippocampal slices by modulating the sodium channel.[3] The dual Toll-like receptor 7/8 antagonist had the potential to treat autoimmune diseases.[4] 5-Pyridonyl-indazole derivative exhibits good sphingosine-1-phosphate receptor 2 (S1P2) inhibitory activity and *in vivo* anti-idiopathic pulmonary fibrosis potency.[5] The N-myristoyl transferase inhibitors with this scaffold achieve the full cures in a mouse model of African

* Corresponding authors. E-mail: jiangyuqin@htu.edu.cn; bingyu@zzu.edu.cn; 2016007@htu.edu.cn
Received August 28, 2022; revised October 13, 2022; published online November 7, 2022.
Project supported by the National Natural Science Foundation of China (Nos. 82003585, 21971224), the Technical Innovation Team of Henan Normal University (No. 2022TD03) and the National College Students' Innovation and Entrepreneurship Training Program of China (No. 202210476076).
国家自然科学基金(Nos. 82003585, 21971224)、河南师范大学优秀科技创新团队(No. 2022TD03)及中国国家级大学生创新创业训练计划(No. 202210476076)资助项目.

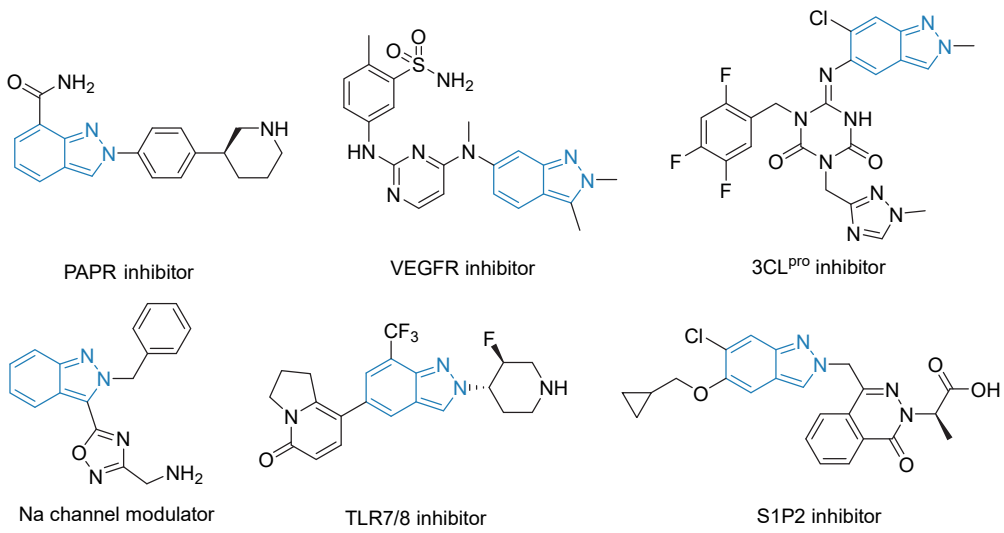

Figure 1 Bioactive compounds with 2*H*-indazole scaffold

sleeping sickness.[6] Owing to their importance, the direct functionalization of 2*H*-indazoles becomes highly desirable to medicinal chemistry and organic chemistry.

The past two decades have witnessed the growth of the synthesis of functionalized heterocycles.[7-17] Particularly, a lot of novel methods to construct the 2*H*-indazole derivatives were developed through direct C—H functionalization. In 2020, Hajra's group[18] reviewed the direct derivation of indazoles. Very recently, the same group[19] updated the latest progress in the field of visible light-mediated functionalization of indazoles and pyrazoles. However, the review customized for the direct functionalization of 2*H*-indazole, especially by the sustainable strategy, is rare. Compared with the traditional thermal procedures, such as transition metal catalyzed C—H activation or $AgNO_3$/$Na_2S_2O_8$ system, photocatalysis and electrocatalysis represent greener protocols and are widely applied in organic transformations. Photocatalytic synthesis uses renewable visible light to initiate the radical reaction to replace high-temperature heating.[20-25] Electrocatalysis is another common and environmentally friendly platform for redox-mediated transformation in organic synthesis.[26-29] It has the advantages of convenience, environmental sustainability, and controllability by changing potential, current or total charge. This review summarizes the visible-light-promoted and electrochemical functionalization of 2*H*-indazole and the corresponding catalytic systems.

2 The photocatalysis strategy

2.1 Rose bengal catalytic system

In 2018, Hajra and his co-authors[30] employed the rose Bengal (RB)/1,5-dizzabicyclo[5.4.0]undecen-5-ene (DBU) organophotoredox system to achieve the C3-phosphonylation of 2*H*-indazoles (Scheme 1). The optimized reaction conditions are established as follows: 2*H*-indazole was reacted with 1.5 equiv. of diphenylphosphine oxide in the presence of 3 mol% rose bengal as the photocatalyst, 2.0 equiv. of DBU as the base, CH_3CN/H_2O (1.0/0.18 mL) as the mixture solvent irradiated with 34 W blue LED for 16 h. When the catalyst RB is replaced by eosin Y or eosin B, the yields of the desired product were dramatically decreased. The protocol has the advantage of being metal-free, aerobic oxidation and scalable. The primary mechanistic research shows that the free radical scavengers, such as 2,2,6,6-tetramethyl- piperidine-1-oxyl (TEMPO), 2,6-di-*tert*-butyl-4-methyl phenol (BHT) and *p*-benzoquinone (BQ), completely inhibit the reaction, indicating that a free radical pathway is involved in this process. A plausible mechanism is proposed. After absorbing a photon from the blue LED, RB is transformed into its excited-state RB*. It is reductively quenched by 2-phenyl-2*H*-indazole to generate the radical anion $RB^{\bullet-}$ along with the indazole radical cation via a single electron-transfer (SET) process. The radical anion $RB^{\bullet-}$ is oxidated by O_2 in the air to regenerate RB and yield the highly active superoxide radical anion ($O_2^{\bullet-}$). Then hydrogen atom transfer (HAT) occurs between $O_2^{\bullet-}$ and diphenylphosphine oxide to form the phosphoryl radical and HO_2^-. The coupling of phosphoryl radical and indazole radical cation is followed by a deprotonation process to deliver the final product.

In 2019, the same group[31] reported an organophotocatalyzed C(sp^2)—C(sp^3) dehydrogenation coupling reaction using rose bengal/triethylene diamine (DABCO)/*tert*-butyl hydrogen peroxide (TBHP) catalytic system (Scheme 2). Using this system, 2*H*-indazole with electron-donating groups or halogen could smoothly react with ethers, such as tetrahydrofuran (THF), 1,3-dioxolane, 2-methyltetrahydrofuran, 1,4-dioxane, diethyl ether and tetrahydrothiophene. Rose bengal plays an essential role in this protocol. No or trace desired products were detected in the absence of catalyst or replacement with eosin Y, eosin B, rhodamine 6G and $Ir(ppy)_3$. Moreover, the alkoxyalkyl radical adduct trapped by the scavenger was successfully isolated. It is proposed that TBHP accepts a single electron from the excited state RB* to generate a *tert*-butyloxy rad-

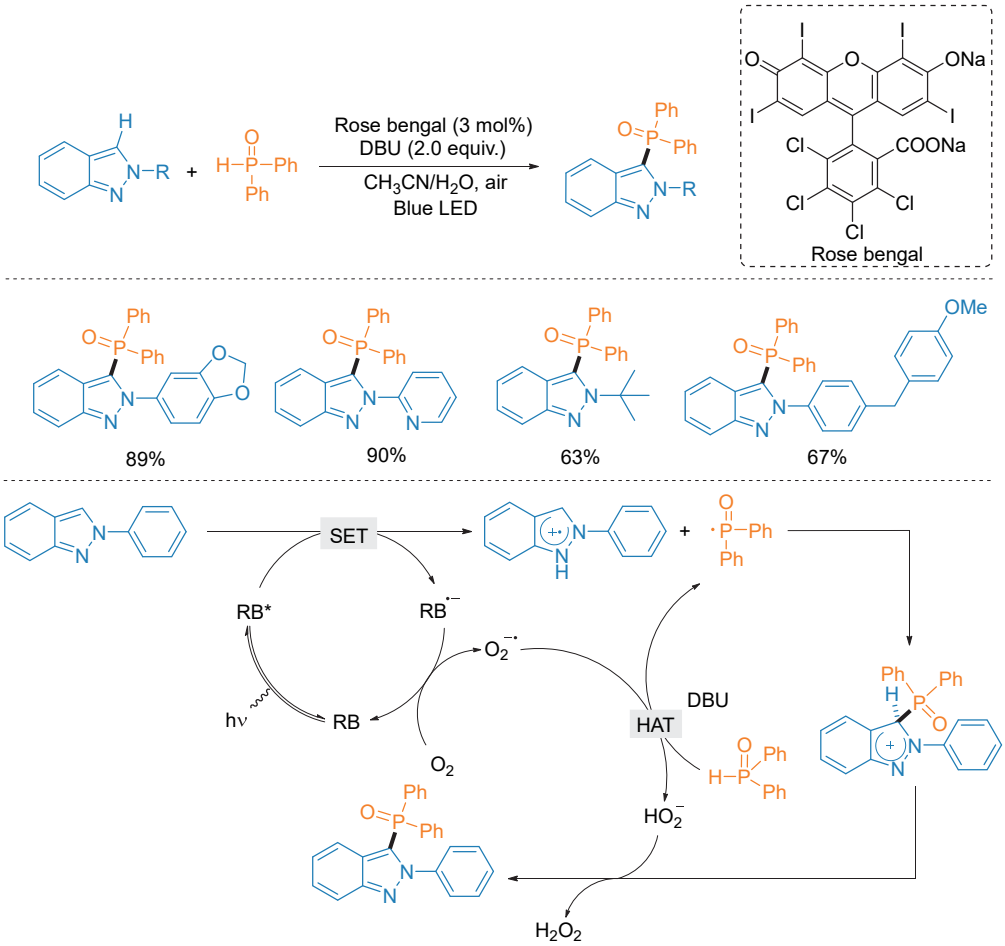

Scheme 1 C3-Phosphonylation of 2*H*-indazoles

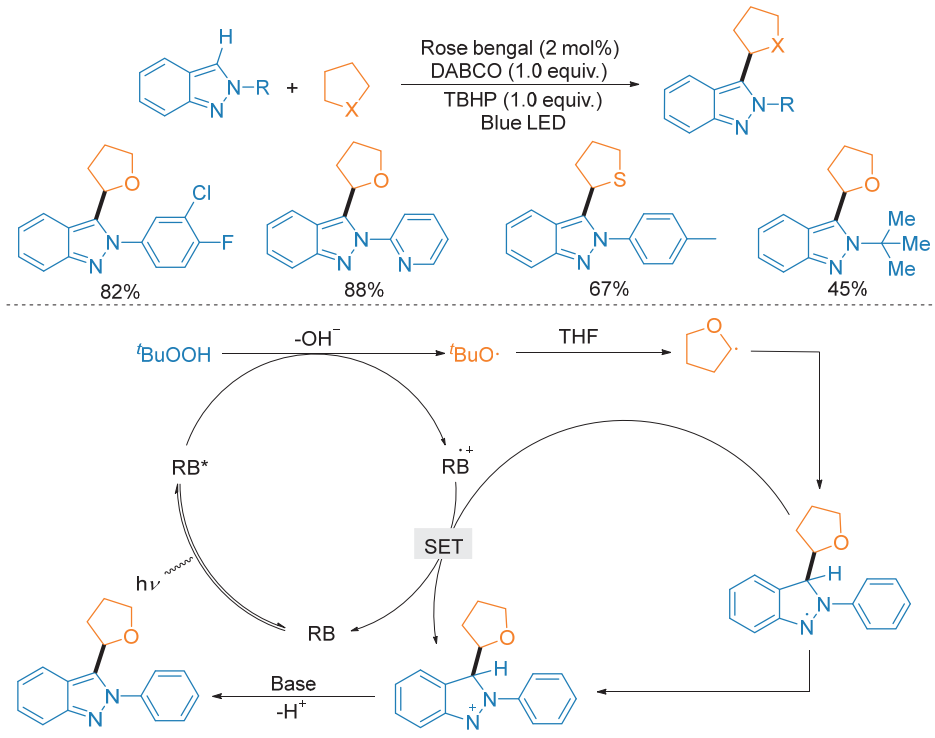

Scheme 2 C3-Oxyalkylation of 2*H*-indazoles

ical. Then *tert*-butyloxy radical and THF undergoes a HAT process to produce the key alkoxyalkyl radical.

2.2 Methylene blue catalytic system

Sharada and Bakthadoss's group[32] reported a methylene blue/phenyliodine diacetate (PIDA) system to construct C3-trifluoromethylation of 2*H*-indazole (Scheme 3). The transition-metal-free photoredox catalysis method uses cheap and stable Langlois reagent as the source of CF_3, the 60 W compact fluorescent bulb as the light source, and dichloromethane (DCM) as the solvent. Rose bengal could also be used in the protocol, giving the desired product in 60% yield. Based on the control experiments and cyclic voltammetry (CV) experiments, a plausible radical-involved reaction mechanism is provided. The visible light initiates the reaction by providing a photon to the photocatalyst (PC) methylene blue. The excited-state PC* generated from the above process oxidates the 2*H*-indazole to give the corresponding radical cation via a SET process. The indazole radical cation reacts with the trifluoromethyl radical which is generated from $NaSO_2CF_3$ by the oxidation of PIDA, and then undergoes deprotonation to yield the target product.

2.3 Acr^+-$MesClO_4$ catalytic system

9-Mesityl-10-methylacridinium perchlorate (Acr^+-$MesClO_4$) was used as the photocatalyst in the C3-amination of 2*H*-indazole by Hajra's group[33] (Scheme 4). The screening of the photocatalysts indicates that eosin Y, rhodamine 6G, rose bengal, and $Ru(bpy)_3Cl_2$ are not suitable for this reaction. Under the irradiation of 34 W blue LED, a variety of amines including secondary amine, aliphatic primary

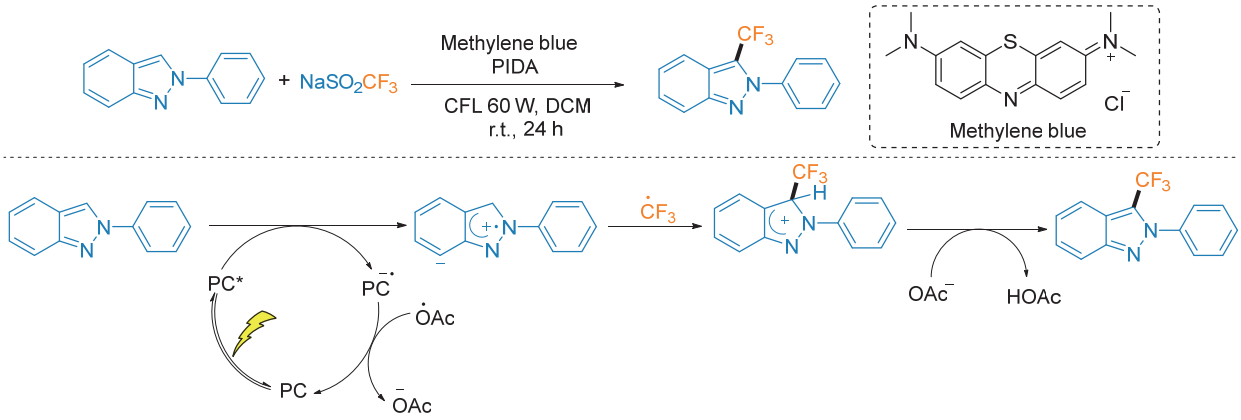

Scheme 3 C3-Trifluoromethylation of 2*H*-indazoles

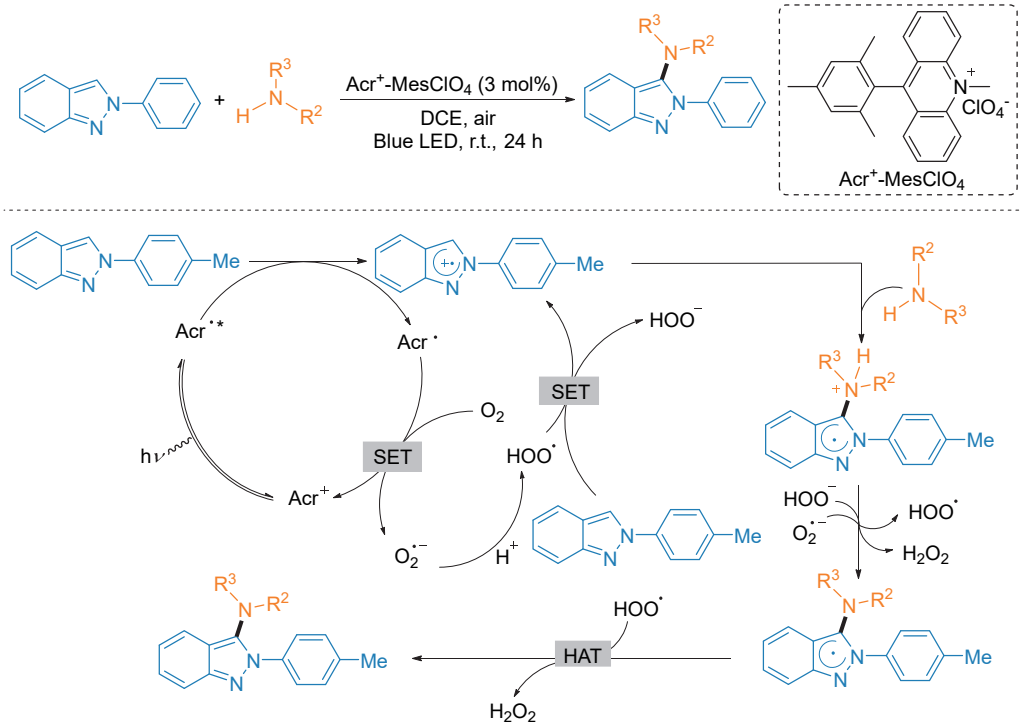

Scheme 4 C3-Amination of 2*H*-indazoles

amine, azole, and sulfoximines could be directly introduced into 2*H*-indazoles through C(sp^2)—N dehydrogenation coupling reaction. On the other hand, aniline, dibenzylamine and diphenylamine failed to act as amine sources in this system. Based on the results of the CV and fluorescence quenching experiment, the Acr* [$E_{1/2}$(PC*/ PC$^-$)= 1.86 V] is presumed to be oxidatively quenched by 2*H*-indazole (E_{ox}=1.04 V). This SET process yields the key indazole radical cation and starts the reaction. The O_2 in air oxidates the Acr• and closes the photoredox cycle. The indazole radical cation is coupled with amine, which is followed by dehydrogenation and hydrogen atom transfer (HAT) to give the final product.

In 2021, Li's group[34] explored a transition metal-free, visible light-mediated C(sp^2)—O coupling reaction between 2*H*-indazoles and alcohols in the presence of Acr$^+$-$MesClO_4$ as the photocatalyst and Selectfluor as the oxidant (Scheme 5). It was found that the reaction efficiency of the linear primary alcohol was satisfactory. It is worth noting that the yield decreases with the increase of alkyl chain length. Primary and secondary alcohols with branched chains and cyclic secondary alcohols are also suitable substrates and react smoothly under standard conditions to generate the desired products in 79%～88% yields. However, tertiary alcohols, benzyl alcohol and phenol cannot be applied in this system. The initiation of the reaction is as same as that of Hajra's report. However, the completion of the photocatalytic cycle relies on Selectfluor, rather than O_2.

2.4 Eosin Y catalytic system

Kim's group[35] disclosed a continuous-flow organophotocatalytic method to access the C3-arylated 2*H*-indazoles (Scheme 6). After the screening of reaction conditions in the batch reactor, the optimal conditions were established as follows: 1 equiv. of 2*H*-indazole and 2 equiv. of phenyl diazonium tetrafluoroborate as the starting materials, 3 mol% eosin Y as the photocatalyst, 1 equiv. DIPEA as the

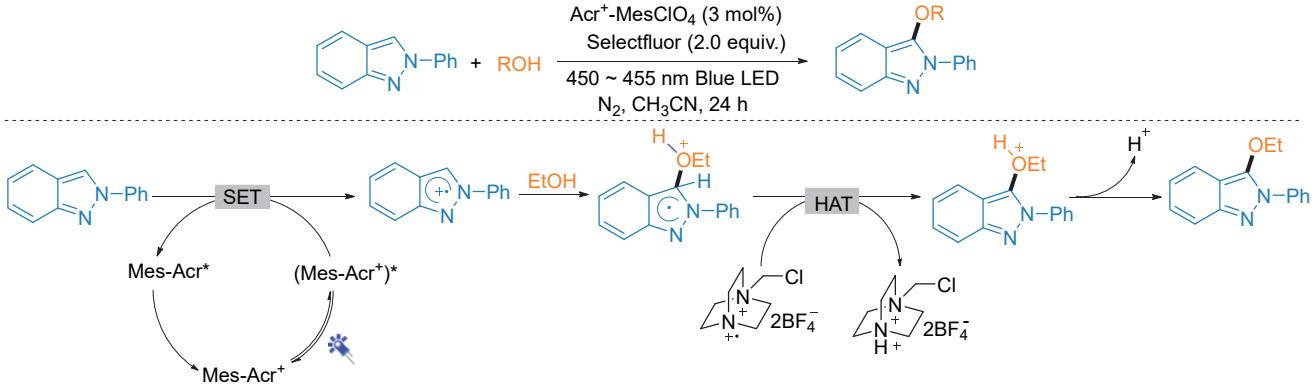

Scheme 5 C3-Alkoxylation of 2*H*-indazoles

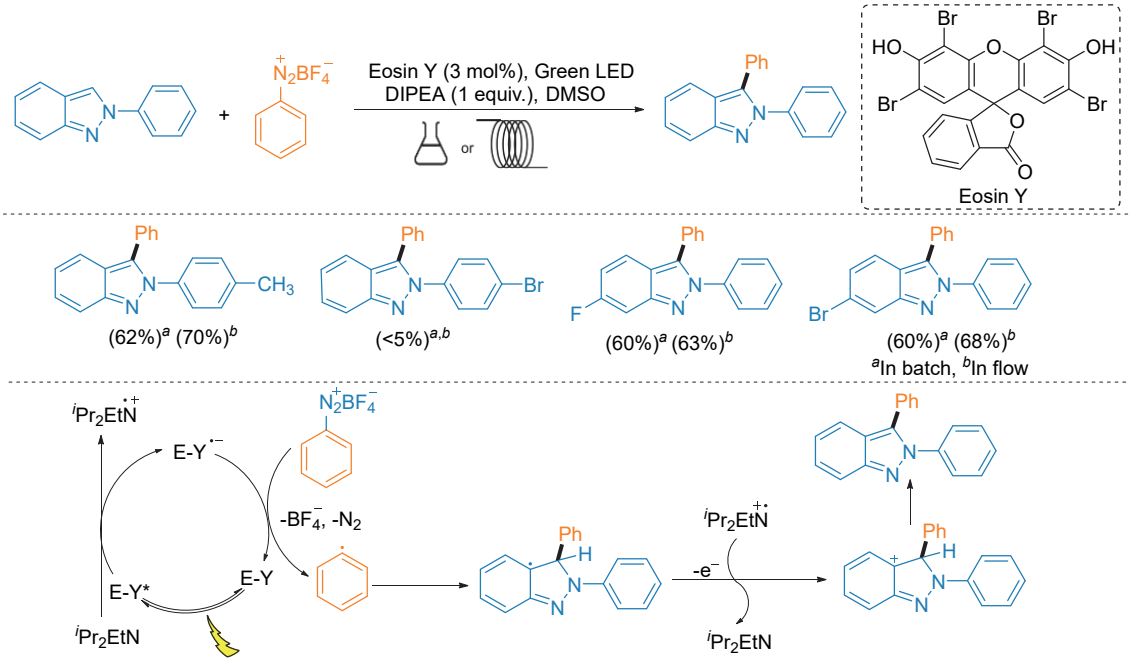

Scheme 6 C3-Arylation of 2*H*-indazoles

base, and 2 mL of dimethyl sulfoxide (DMSO) as the solvent. When the conventional reactor was replaced by a continuous flow microfluidic reactor, which could provide efficient visible light irradiation and intensive mixing, the yield of the desired product was surprisingly improved from 65% to 74%. Meanwhile, the reaction time was significantly decreased from 18 h to 1 min. Moreover, liver X-receptor inhibitors could be rapidly synthesized with this green method. The result of the radical trapping experiment indicates that a free radical pathway may be involved in the reaction. In the proposed mechanism, the excited state eosin Y* is converted into the reduced state eosin $Y^{\bullet-}$ by a SET process from DIPEA. Another SET occurs between the eosin $Y^{\bullet-}$ and phenyl diazonium tetrafluoroborate, affording the aryl radical and completing the catalytic cycle.

2.5 4CzIPN catalytic system

In 2021, Ramesh's group[36] reported a 1,2,3,5-tetrakis(carbazol-9-yl)-4,6-dicyanobenzene (4CzIPN) catalyzed directly arylation of 2*H*-indazole (Scheme 7). Different from Kim's method[35], more safe and easily available anilines were used as aryl radical sources. It was found that the reaction yield was related to the amount of the photocatalyst. For example, 10 mol% 4CzIPN promoted the reaction to obtain the required product with 80% yield, while 2 mol% 4CzIPN as the photocatalyst did not obtain any product. The gram-scale reaction was also successful. Moreover, the photocatalyst could be recovered by silica gel column chromatography and recycled in the next photoactivated transformation. A series of control experiments were conducted to investigate the reaction pathway. Notably, TEMPO trapped aryl radical species were detected in the radical trapping experiments. Based on the results, it is believed that aniline reacts with *tert*-butyl nitrite to *in situ* generate the diazonium salt. It obtains a single electron from the reduced $4CzIPN^{\bullet-}$ to deliver the key aryl radical.

In the same year, our group[37] realized the direct C3-alkylation of 2-aryl-2*H*-indazole through a 4CzIPN-catalyzed decarboxylative $C(sp^2)$—$C(sp^3)$ coupling reaction (Scheme 8). In the presence of alkyl *N*-hydroxyphthalimide esters (NHPE) as alkylating reagents, dimethyl carbonate as a green solvent, triethylenediamine (DABCO) as a base, various primary, secondary and tertiary alkyl groups were introduced into the C3 position of 2*H*-indazoles. Moreover, this visible-light-mediated protocol can be used in the late-stage modification of drugs including dehydrocholic acid and gemfibrozil, and the construction of novel unnatural amino acids. The influence of the reaction parameters is exhibited in a radar diagram, which indicates that the oxygen atmosphere completely inhibits the reaction, and the light intensity and catalyst dosage are well-tolerant. The proposed mechanism is shown as Scheme 8. The excited state 4CzIPN* is quenched by DABCO, which is confirmed by the result of fluorescence quenching and CV experiments. Through a SET procedure, the reduced state $4CzIPN^{-}$ was oxidated by NHPE to complete the catalytic cycle. The NHPE radical anions generated from the above process undergo fragmentation to afford the key alkyl radical. Then 2*H*-indazole reacts with alkyl radicals to obtain N-3-alkyl-2-phenyl-indazole

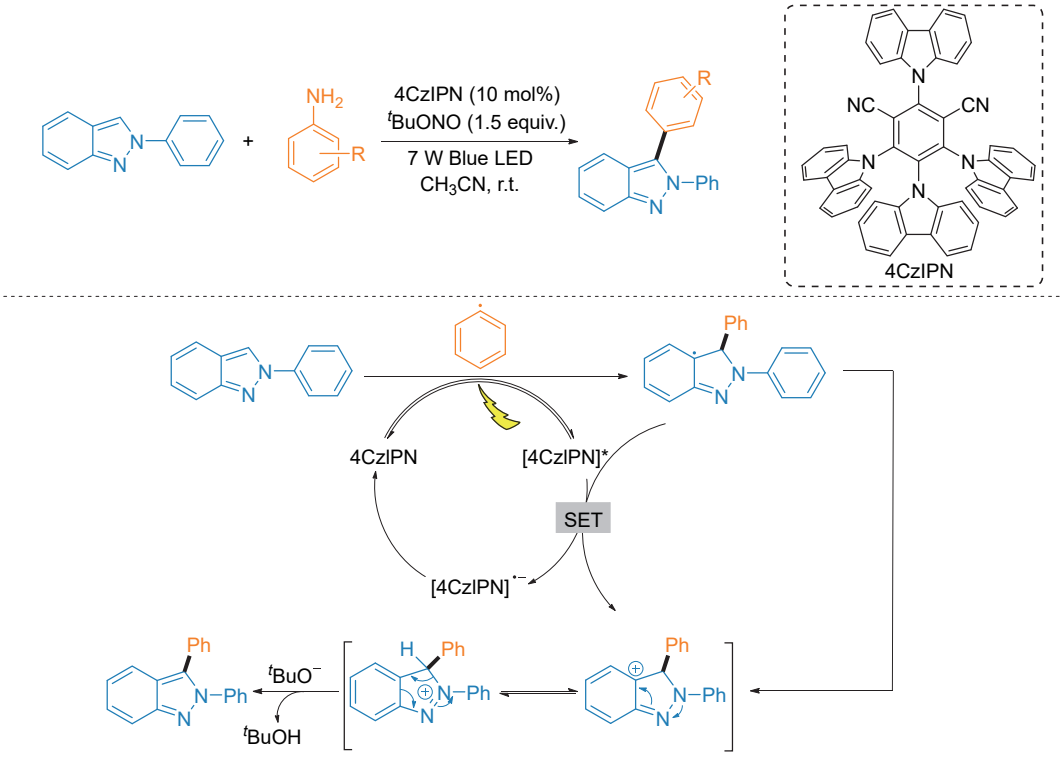

Scheme 7 4CzIPN-catalyzed C3-arylation of 2*H*-indazoles

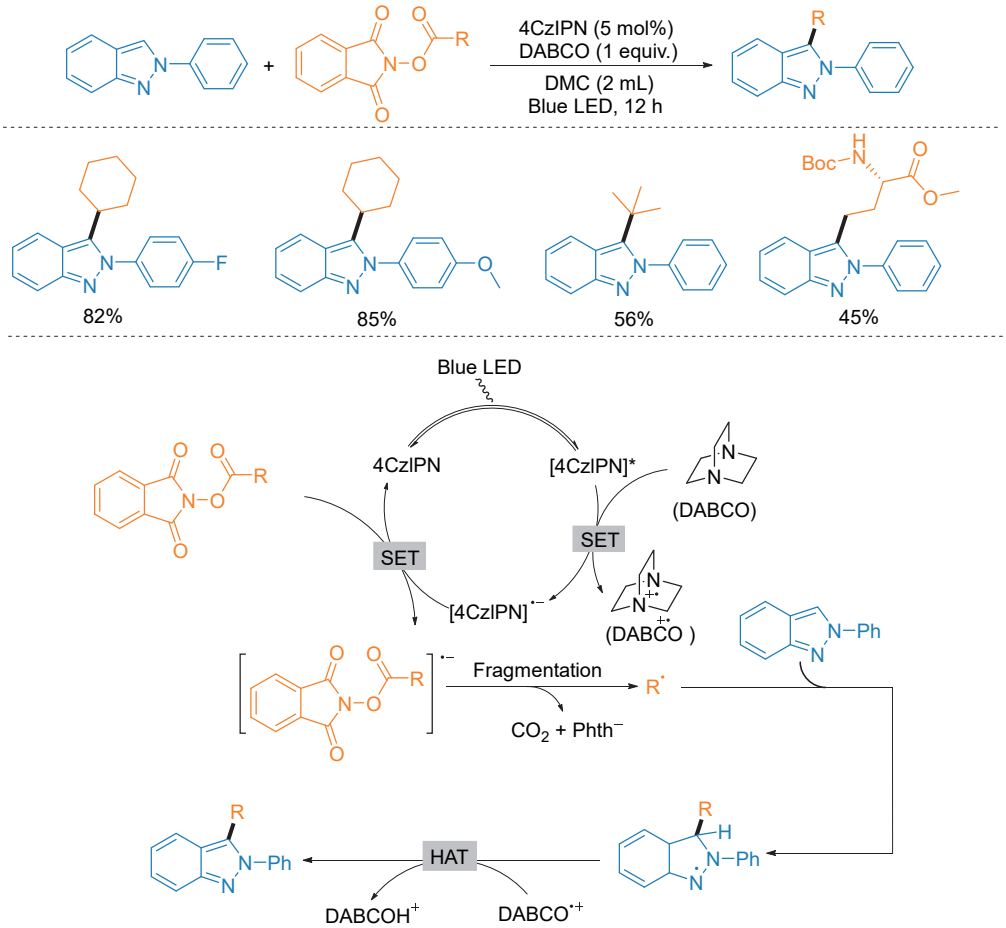

Scheme 8 C3-Alkylation of 2*H*-indazoles

radical intermediate. A hydrogen atom transfer reaction (HAT) is occurred between the radical intermediate and $DABCO^{\bullet+}$ to obtain the target products.

In 2021, Ramesh and his coworkers[38] achieved the C3-arylation of 2*H*-indazoles using phenylhydrazine hydrochloride as the aryl source and 4CzIPN as the photocatalyst (Scheme 9). The scope investigation of this oxidative coupling reaction indicated that the electron-withdrawing groups in the phenylhydrazine hydrochloride, especially CN and NO_2, are beneficial to the reaction, while the electron-donating groups lowered the yields. The position of substitutions drastically influenced the reaction yields, revealing that the steric hindrance in the phenyl radical sources must be taken into consideration in the application of this strategy. *N*-Phenyl indazoles with different substitutions and *N*-benzyl indazole were tolerant, while the *N*-aliphatic indazole failed to deliver the desired product. The protocol was successfully applied in the construction of the liver X receptor agonist. The control experiments indicated that photocatalyst, base, visible light and oxygen molecule play important roles in the reaction. The radical trapping experiments demonstrated that an aryl radical is involved in the reaction. A plausible mechanism provided by the authors is shown in Scheme 9. The phenylhydrazine hydrochloride was converted into the aryl radical in the presence of a base and oxygen molecule. The radical underwent homolytic aromatic substitution and oxidization to afford the desired products.

2.6 Rhodamine B catalytic system

Recently, our group[39] developed a rhodamine B/dilauroyl peroxide (DLP) catalytic system to achieve the 3-ethoxycarbonylmethylation of 2*H*-indazole in green solvent water (Scheme 10). In this visible-light-driven strategy, commercially available *α*-bromoesters are used as the coupling source, rather than traditional agents including xanthate esters or ethyl diazoacetate. Moreover, the valuable pharmacophore *α*-bromoamides are also applicable to the method. The method could be used in the late-stage modification of natural products and the synthesis of the drug Zolpidem in a one-pot manner. The radar diagram of the sensitivity experiment indicates that the reaction can adapt to most parameters variation, in favor of the application in the pharmaceutical and chemical industry. After a series of control experiments and Stern-Volmer fluorescence quenching experiments, the *in situ* generated xanthate ester is involved in the reaction by providing the key alkyl radical.

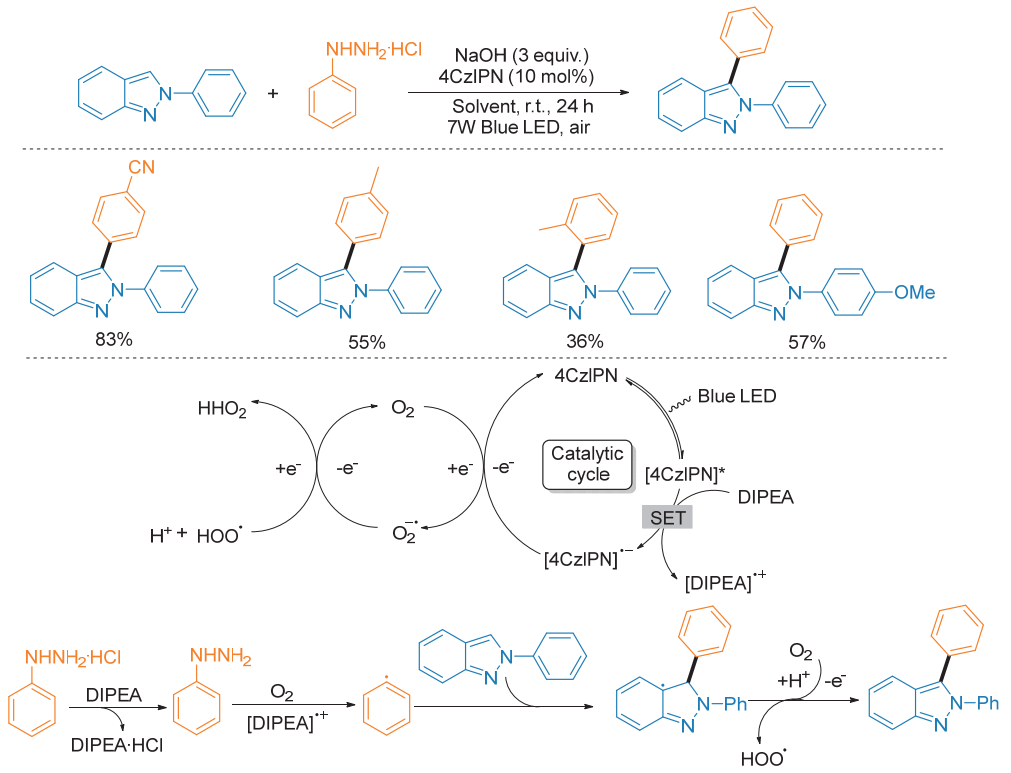

Scheme 9 C3-Arylation of 2*H*-indazoles

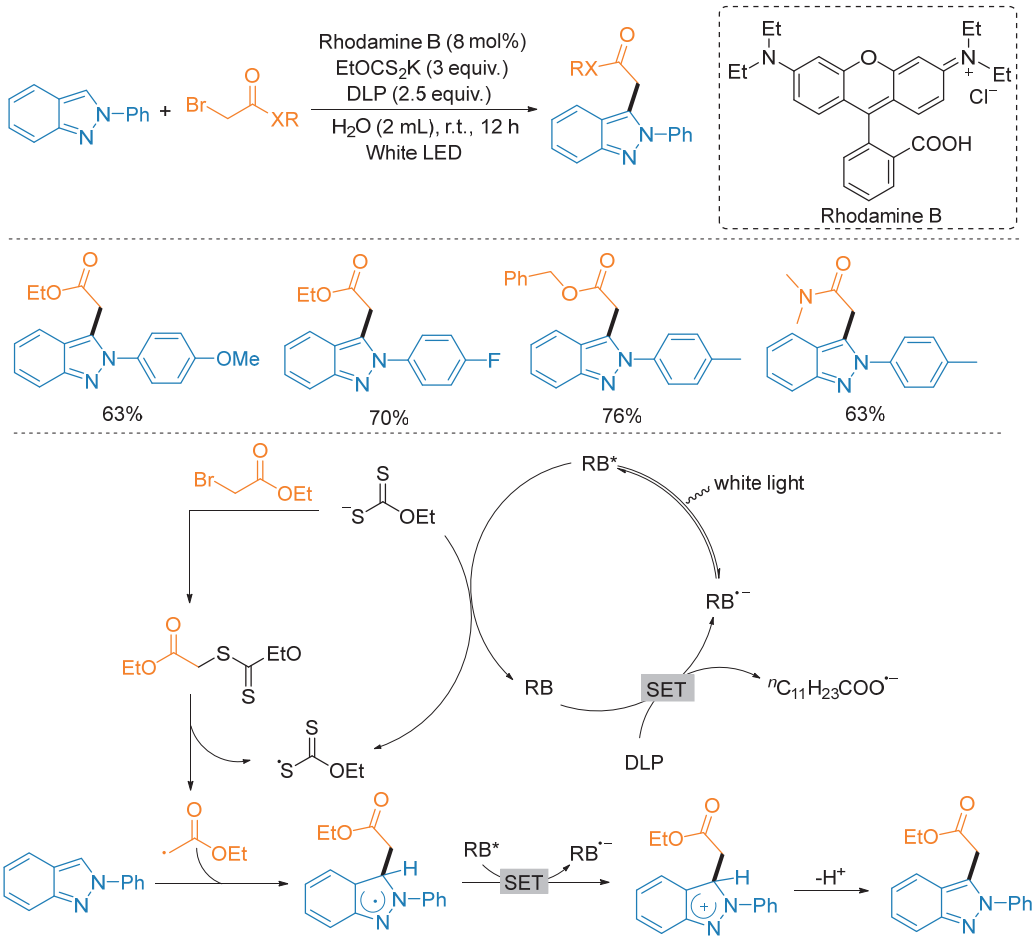

Scheme 10 C3-Ethoxycarbonylmethylation of 2*H*-indazoles

2.7 Electron-donor-acceptor (EDA) complex catalytic system

Electron-donor-acceptor (EDA) complex system represents a novel photocatalytic system without using transition metal catalysts and traditional organic dyes. Lee's group[40] reported a visible-light-mediated, EDA complex catalyzed method to access the C3-arylated-2*H*-indazoles in the presence of aryl diazonium salts as the aryl radical source, pyridine as the base, and DMSO as the solvent under N_2 (Scheme 11). The control experiment indicates that the aryl radical which could be trapped by TEMPO is involved in the reaction. The clear bathochromic shift observed in the UV-vis spectroscopy of the reaction components mixture demonstrates that a ternary EDA complex was formed among 2*H*-indazole, aryldiazonium salt, and pyridine. It is presumed that the EDA complex is excited by the blue LED and triggers the formation of the aryl radical.

3 Electrocatalysis strategy

3.1 $LiClO_4$ electrolyte involved system

Oh's group[41] reported a radical-radical cross-coupling strategy for C(sp^2)—S bond formation to achieve the direct 3-sulfonylation of 2*H*-indazole under electrochemical conditions (Scheme 12). This redox-reagent-free approach employs sodium sulfinates as the green sulfonyl radical

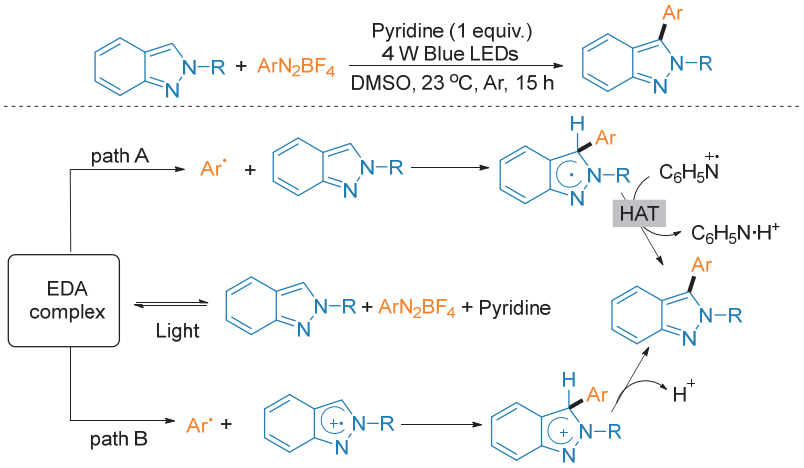

Scheme 11 C3-Arylation of 2*H*-indazoles enabled by the EDA system

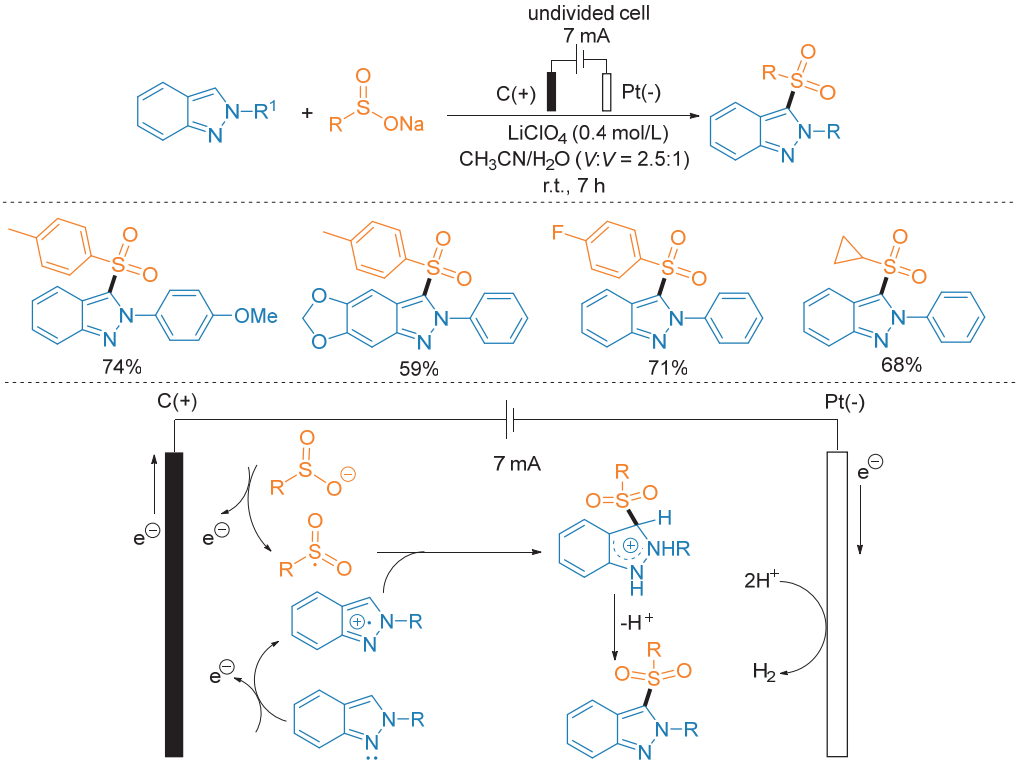

Scheme 12 Electrochemical C3-sulfonylation of 2*H*-indazoles

source, $LiClO_4$ as the electrolyte, an undivided cell containing graphite anode, and platinum as the cathode. Various 2*H*-indazoles react well in this system, except for the derivatives with the *tert*-butyl or nitro group. In the scope of sodium sulfinates, nitro-substitution is also unfavorable in the protocol. According to the result of the CV experiment, the close oxidation potentials between 2*H*-indazoles and sulfinates may be crucial to the success of the reaction. It is proposed that both 2*H*-indazoles and sulfinates are anodically oxidated to generate the sulfonyl radical and indazole radical cation. The desired product is obtained by a radical-radical cross-coupling process and deprotonation. The electrochemical cycle is finished by the reduction of protons to hydrogen gas on the cathode.

In the same year, De Sarkar's group[42] discovered the direct C3-sulfonylation of 2*H*-indazoles using sulfonyl hydrazides as the sulfonyl radical precursor by a similar catalytic system (Scheme 13). The practical and scalable protocol has the potential for application in the industry. In the presence of K_2CO_3, sulfonyl hydrazide is oxidated on the anode surface and then undergoes nitrogen evolution to give a sulfonyl radical. Subsequently, the sulfonyl radical adds to the indazole, then undergoes one-electron oxidation and deprotonation aromatization to afford the target product.

3.2 $^{n}Bu_4NBF_4$ electrolyte involved system

Li and Wang's group[43] developed a concise and efficient electrochemical procedure for the C-3 amination of 2*H*-indazoles in the presence of $^{n}Bu_4NBF_4$ as the electrolyte (Scheme 14). This protocol applies a platinum electrode as a cathode, a graphite rod as an anode, and CH_3CN as a solvent at a constant current of 5 mA for 3 h. When the aromatic ring of 2-phenyl 2*H*-indazole contains an electron-donating group or an electron-withdrawing group at the *meta*- or *ortho*-position, the desired products could be obtained in good yields, indicating that there are no obvious steric hindrance effects or electronic effects in this electrically driven reaction. The commercially available azoles (pyrazoles with various substitutions, triazole, tetrazolium, benzimidazole, and benzotriazole) and aliphatic amines (morpholine and n-butylamine) could be used as amination reagents. In the proposed reaction mechanism, 2*H*-indazole is oxidated on the anode to generate the indazole radical cation, which then reacts with azole to give the final product through anode oxidation and deprotonation.

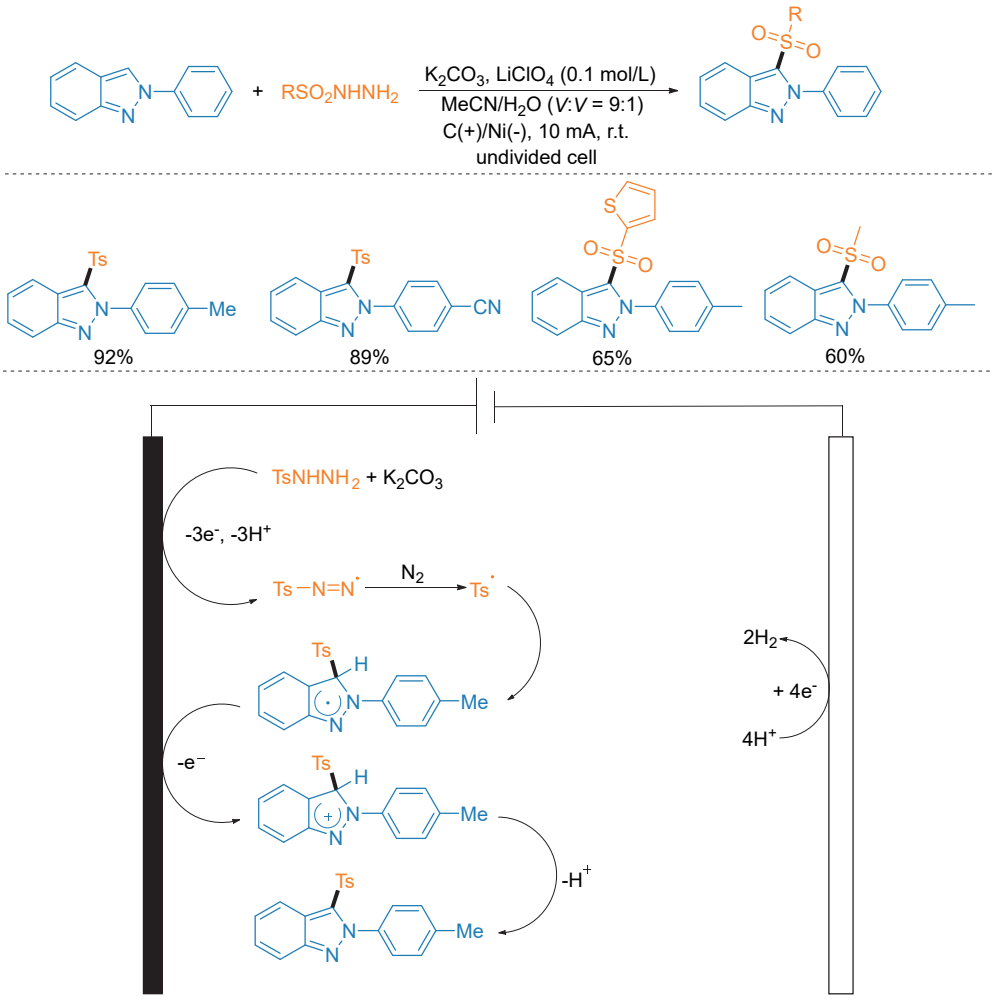

Scheme 13 C3-Sulfonylation of 2*H*-indazoles using sulfonyl hydrazides

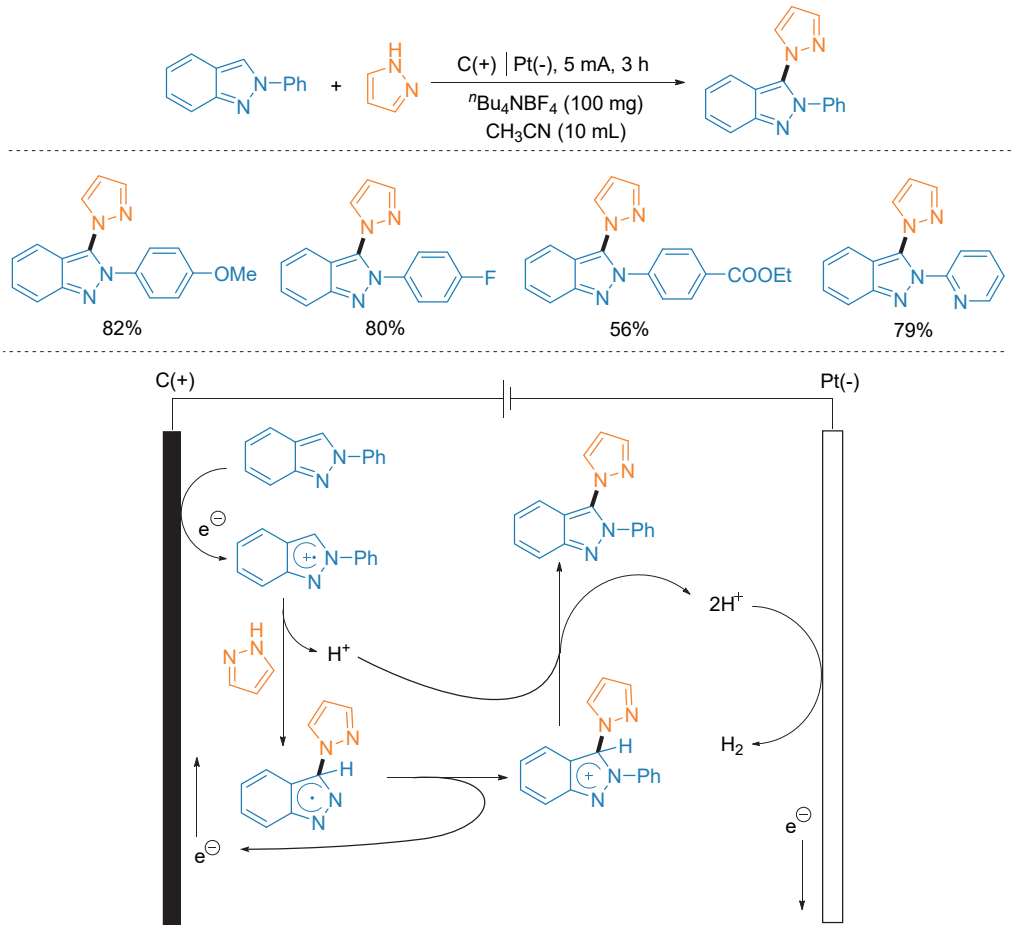

Scheme 14 Electrochemical C3-amination of 2*H*-indazoles

Xie's group[44] employed the same catalytic system to achieve the transition-metal-free, oxidant-free trifluoromethylation of 2*H*-indazoles (Scheme 15). The 2-phenyl-2*H*-indazoles with various functional groups are converted into the anticipated products in the presence of CF_3SO_2Na as the CF_3 source, a catalytic amount of ^{n}Bu$_4$NBF$_4$ as the electrolyte, and MeCN as the solvent. The anodic oxidation, radical-radical coupling, and proton transfer may play an essential role in the reaction process.

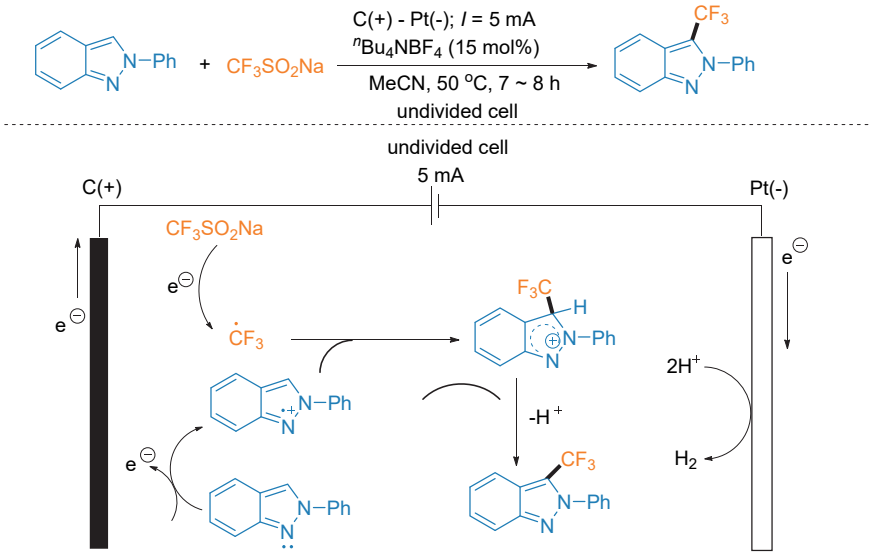

Scheme 15 C3-Trifluoromethylation of 2*H*-indazoles

3.3 $^{n}Bu_4NPF_6$ electrolyte involved system

In accordance with the regioselective protocol reported by Ruan *et al.*[45] in 2022, various diselenides could be inserted into the C3-position of 2*H*-indazole via an electrochemical procedure (Scheme 16). The heterocycles including 1-phenyl-1*H*-pyrazole and imidazo[1,2-*α*]pyridines are found to be suitable substrates. Meanwhile, the diaryl diselenides and aliphatic diselenides are suitable selenium sources in this reaction. PhSeSePh has converted into selenium radical and selenium cation by anodic oxidation. There may be two pathways to initiate the reaction. On one hand, the radical adds to the 2*H*-indazole to form the radical intermediate, which is then oxidation deprotonated to give the desired product. On the other hand, the addition of the selenium cation to 2-phenyl-2*H*-indazole produces the PhSe-indazole cationic intermediate. It is subsequently deprotonated to afford the target product.

4 Conclusions

In this review, the recent advances in the direct C-3 functionalization of 2*H*-indazoles for the construction of C—P, C—C, C—N, C—O and C—Se bonds under photochemical and electrochemical conditions were summarized according to the catalytic systems. Generally, most of the reported methods worked well without high-temperature heating, strong oxidants, or transition metals. Compared with the classic transition metal-catalyzed cross-coupling reactions including the Heck reaction, Suzuki reaction, and Sonogashira reaction, these photocatalytic and electrochemical strategies show high regioselectivity and step-/atom-economy without the preactivation of substrates. On the other hand, it should be noted that there are some differences between the photocatalytic strategies and electrochemical strategies based on the above-mentioned catalytic systems. Firstly, the photocatalytic reactions usually occur in a homogeneous solution, while the electrochemical systems generated the radical intermediates on the interface of the electrode and solution. In this context, the concentration of radical intermediates in photocatalytic reactions is generally lower than that of the electrochemical systems. Therefore, photocatalytic reactions generally require a longer reaction time than electrochemical systems. Secondly, stoichiometric oxidants are needed in some photocatalytic systems, which could be avoided in the electrochemical systems because the key oxidation step could be realized on the anode. Considering the important role of 2*H*-indazoles in medicinal chemistry, developing green strategies to direct introduce other valuable groups into 2*H*-indazoles is still desirable. We believe that the visible-light-induced and electrochemical protocols will be extensively used in drug discovery and chemical engineering.

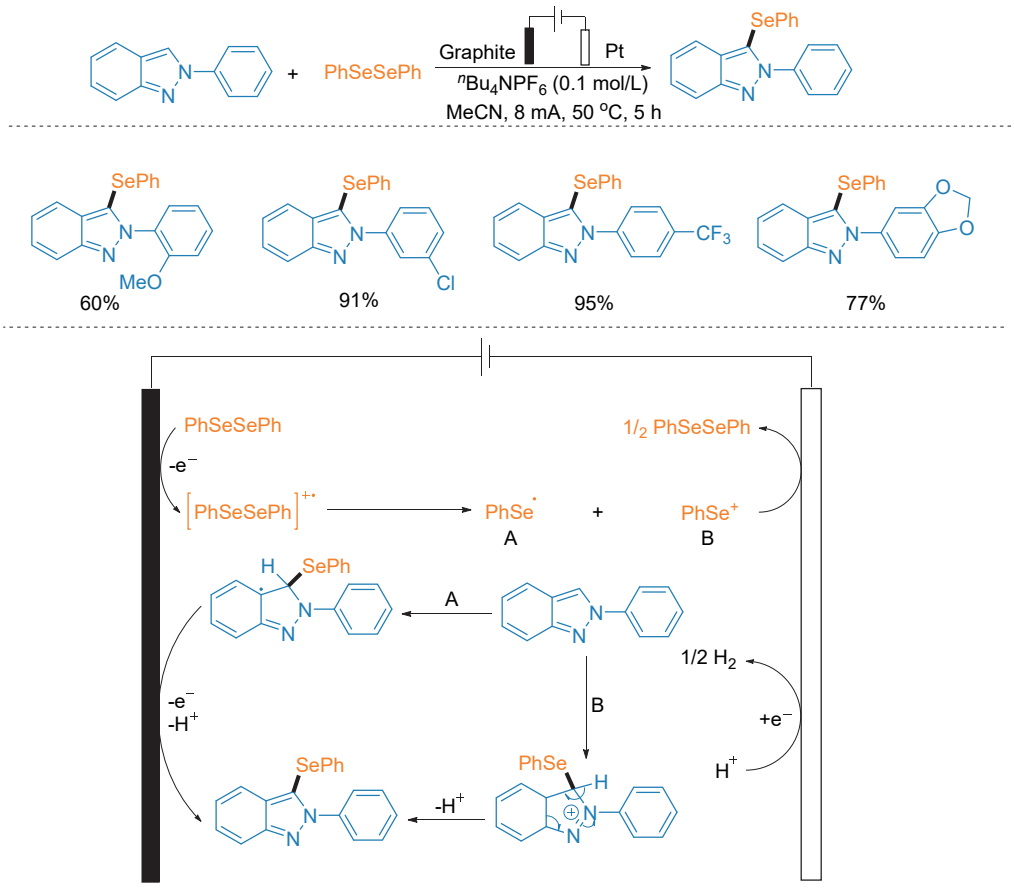

Scheme 16 C3-Selenylation of 2*H*-indazoles

References

[1] Jones, P.; Altamura, S.; Boueres, J.; Ferrigno, F.; Fonsi, M.; Giomini, C.; Lamartina, S.; Monteagudo, E.; Ontoria, J. M.; Orsale, M. V.; Palumbi, M. C.; Pesci, S.; Roscilli, G.; Scarpelli, R.; Schultz-Fademrecht, C.; Toniatti, C.; Rowley, M. *J. Med. Chem.* **2009**, *52*, 7170.

[2] Harris, P. A.; Boloor, A.; Cheung, M.; Kumar, R.; Crosby, R. M.; Davis-Ward, R. G.; Epperly, A. H.; Hinkle, K. W.; Hunter, R. N.; Johnson, J. H.; Knick, V. B.; Laudeman, C. P.; Luttrell, D. K.; Mook, R. A.; Nolte, R. T.; Rudolph, S. K.; Szewczyk, J. R.; Truesdale, A. T.; Veal, J. M.; Wang, L.; Stafford, J. A. *J. Med. Chem.* **2008**, *51*, 4632.

[3] Clutterbuck, L. A.; Posada, C. G.; Visintin, C.; Riddall, D. R.; Lancaster, B.; Gane, P. J.; Garthwaite, J.; Selwood, D. L. *J. Med. Chem.* **2009**, *52*, 2694.

[4] Knoepfel, T.; Nimsgern, P.; Jacquier, S.; Bourrel, M.; Vangrevelinghe, E.; Glatthar, R.; Behnke, D.; Alper, P. B.; Michellys, P.-Y.; Deane, J.; Junt, T.; Zipfel, G.; Limonta, S.; Hawtin, S.; Andre, C.; Boulay, T.; Loetscher, P.; Faller, M.; Blank, J.; Feifel, R.; Betschart, C. *J. Med. Chem.* **2020**, *63*, 8276.

[5] Mammoliti, O.; Jansen, K.; El Bkassiny, S.; Palisse, A.; Triballeau, N.; Bucher, D.; Allart, B.; Jaunet, A.; Tricarico, G.; De Wachter, M.; Menet, C.; Blanc, J.; Letfus, V.; Rupčić, R.; Šmehil, M.; Poljak, T.; Coornaert, B.; Sonck, K.; Duys, I.; Waeckel, L.; Lecru, L.; Marsais, F.; Jagerschmidt, C.; Auberval, M.; Pujuguet, P.; Oste, L.; Borgonovi, M.; Wakselman, E.; Christophe, T.; Houvenaghel, N.; Jans, M.; Heckmann, B.; Sanière, L.; Brys, R. *J. Med. Chem.* **2021**, *64*, 14557.

[6] Harrison, J. R.; Brand, S.; Smith, V.; Robinson, D. A.; Thompson, S.; Smith, A.; Davies, K.; Mok, N.; Torrie, L. S.; Collie, I.; Hallyburton, I.; Norval, S.; Simeons, F. R. C.; Stojanovski, L.; Frearson, J. A.; Brenk, R.; Wyatt, P. G.; Gilbert, I. H.; Read, K. D. *J. Med. Chem.* **2018**, *61*, 8374.

[7] Chen, N.; Lei, J.; Wang, Z.; Liu, Y.; Sun, K.; Tang, S. *Chin. J. Org. Chem.* **2022**, *42*, 1061.

[8] Wang, X.; Lei, J.; Liu, Y.; Ye, Y.; Li, J.; Sun, K. *Org. Chem. Front.* **2021**, *8*, 2079.

[9] Zhang, M.-M.; Qu, B.-L.; Shi, B.; Xiao, W.-J.; Lu, L.-Q. *Chem. Soc. Rev.* **2022**, *51*, 4146.

[10] Chen, X. Y.; Zhang, X.; Wan, J.-P. *Org. Biomol. Chem.* **2022**, *20*, 2356.

[11] Shen, J.; Zhang, L.; Meng, X. *Org. Chem. Front.* **2021**, *8*, 6433.

[12] Liu, Z.-K.; Zhao, Q.-Q.; Gao, Y.; Hou, Y.-X.; Hu, X.-Q. *Adv. Synth. Catal.* **2021**, *363*, 411.

[13] Sun, K.; Wang, X.; Li, C.; Wang, H.; Li, L. *Org. Chem. Front.* **2020**, *7*, 3100.

[14] Yang, G.; Xie, X.; Cheng, M.; Gao, X.; Lin, X.; Li, K.; Cheng, Y.; Liu, Y. *Chin. Chem. Lett.* **2022**, *33*, 1483.

[15] Qi, Y.; Gu, X.; Huang, X.; Shen, G.; Yang, B.; He, Q.; Xue, Z.; Du, M.; Shi, L.; Yu, B. *Chin. Chem. Lett.* **2021**, *32*, 3544.

[16] Wu, Y.; Lin, Y.-W.; He, W.-M. *Chin. Chem. Lett.* **2020**, *31*, 2999.

[17] Ma, C.-H.; Ji, Y.; Zhao, J.; He, X.; Zhang, S.-T.; Jiang, Y.-Q.; Yu, B. *Chin. J. Catal.* **2022**, *43*, 571.

[18] Ghosh, S.; Mondal, S.; Hajra, A. *Adv. Synth. Catal.* **2020**, *362*, 3768.

[19] Ghosh, D.; Ghosh, S.; Ghosh, A.; Pyne, P.; Majumder, S.; Hajra, A. *Chem. Commun.* **2022**, *58*, 4435.

[20] Chen, Z.; Xuan, J. *Chin. J. Org. Chem.* **2022**, *42*, 923 (in Chinese).
(陈泽乐, 宣俊, 有机化学, **2022**, *42*, 923.)

[21] Jiang, Y.-Q.; Li, J.; Feng, Z.-W.; Xu, G.-Q.; Shi, X.; Ding, Q.-J.; Li, W.; Ma, C.-H.; Yu, B. *Adv. Synth. Catal.* **2020**, *362*, 2609.

[22] Wang, P.; Zhao, Q.; Xiao, W.; Chen, J. *Green Synth. Catal.* **2020**, *1*, 42.

[23] Qu, C.; Liu, R.; Wang, Z.; Lv, Y.; Yue, H.; Wei, W. *Green Chem.* **2022**, *24*, 4915.

[24] Lv, Y.; Bao, P.; Yue, H.; Li, J.-S.; Wei, W. *Green Chem.* **2019**, *21*, 6051.

[25] Meng, N.; Lv, Y.; Liu, Q.; Liu, R.; Zhao, X.; Wei, W. *Chin. Chem. Lett.* **2021**, *32*, 258.

[26] Meng, Z.; Feng, C.; Xu, K. *Chin. J. Org. Chem.* **2021**, *41*, 2535 (in Chinese).
(蒙泽银, 冯承涛, 徐坤, 有机化学, **2021**, *41*, 2535.)

[27] Li, J.; Zhang, S.; Xu, K. *Chin. Chem. Lett.* **2021**, *32*, 2729.

[28] Yuan, Y.; Lei, A. *Acc. Chem. Res.* **2019**, *52*, 3309.

[29] Xiong, P.; Xu, H.-C. *Acc. Chem. Res.* **2019**, *52*, 3339.

[30] Singsardar, M.; Dey, A.; Sarkar, R.; Hajra, A. *J. Org. Chem.* **2018**, *83*, 12694.

[31] Singsardar, M.; Laru, S.; Mondal, S.; Hajra, A. *J. Org. Chem.* **2019**, *84*, 4543.

[32] Murugan, A.; Babu, V. N.; Polu, A.; Sabarinathan, N.; Bakthadoss, M.; Sharada, D. S. *J. Org. Chem.* **2019**, *84*, 7796.

[33] Neogi, S.; Ghosh, A. K.; Majhi, K.; Samanta, S.; Kibriya, G.; Hajra, A. *Org. Lett.* **2020**, *22*, 5605.

[34] Sun, M.; Li, L.; Wang, L.; Huo, J.; Sun, M.; Li, P. *Org. Chem. Front.* **2021**, *8*, 4230.

[35] Vidyacharan, S.; Ramanjaneyulu, B. T.; Jang, S.; Kim, D.-P. *ChemSusChem* **2019**, *12*, 2581.

[36] Saritha, R.; Annes, S. B.; Ramesh, S. *RSC Adv.* **2021**, *11*, 14079.

[37] Ma, C.; Feng, Z.; Li, J.; Zhang, D.; Li, W.; Jiang, Y.; Yu, B. *Org. Chem. Front.* **2021**, *8*, 3286.

[38] Saritha, R.; Annes, S. B.; Perumal, K.; Veerappan, A.; Ramesh, S. *ChemistrySelect* **2021**, *6*, 12440.

[39] Ma, C.-H.; Zhao, L.; He, X.; Jiang, Y.-Q.; Yu, B. *Org. Chem. Front.* **2022**, *9*, 1445.

[40] Aganda, K. C. C.; Kim, J.; Lee, A. *Org. Biomol. Chem.* **2019**, *17*, 9698.

[41] Kim, W.; Kim, H. Y.; Oh, K. *Org. Lett.* **2020**, *22*, 6319.

[42] Mahanty, K.; Maiti, D.; De Sarkar, S. *J. Org. Chem.* **2020**, *85*, 3699.

[43] Sun, M.; Zhou, Y.; Li, L.; Wang, L.; Ma, Y.; Li, P. *Org. Chem. Front.* **2021**, *8*, 754.

[44] Wei, T.; Wang, K.; Yu, Z.; Hou, J.; Xie, Y. *Tetrahedron Lett.* **2021**, *86*, 153313.

[45] Lin, S.; Cheng, X.; Hasimujiang, B.; Xu, Z.; Li, F.; Ruan, Z. *Org. Biomol. Chem.* **2022**, *20*, 117.

(Zhao, C.)

